Biochimica et Biophysica Acta 900 (1987) 239–248
Elsevier

BBA 73584

A new paramagnetic analogue of cholesterol as a tool for studying molecular interactions of genuine cholesterol

Luc Maurin, Philippe Morin and Alain Bienvenue

Laboratoire de Biologie Physico-chimique (UA 530 CNRS), USTL, F-34060 Montpellier cedex (France)

(Received 26 February 1987)

Key words: Cholesterol analog; Molecular interaction; Filipin; Amphotericin; ESR; Fluorescence

The synthesis of a new paramagnetic (nitroxide) analogue of cholesterol is described. This compound (called CNO) contains a doxyl group in the lateral chain at position 25. Our results show that CNO retains three molecular interactions which characterize authentic cholesterol: (1) It assumes an orientation perpendicular to the phospholipid bilayer with the doxyl group buried in the membrane core, as seen by ESR spectroscopy. (2) It widens the transition temperature of dimyristoylphosphatidylcholine, to the same extent as cholesterol, as measured by Raman and ESR spectroscopies. (3) It interacts with polyene antibiotics, such as amphotericin B and filipin, in the same manner as its model. This was proved on the one hand by the change in fluorescence of self quenched vesicle-entrapped calcein, after dilution in the external medium, provoked by filipin, and on the other hand by fluorescence quenching provoked by cobalt ions entering the vesicles under the influence of amphotericin B. We concluded that CNO, although it has a side chain different from genuine cholesterol, can help to solve many physiologically meaningful questions related to the distribution and movement rate of cholesterol itself.

Introduction

Cholesterol is one of the major components in biological membranes, in some cases 50% of the total lipid content. The exact role of sterols in membrane structure and function remains unclear, in spite of the extensive literature devoted to this topic. For example, there have been many controversies concerning the stoichiometry of lipid-cholesterol complexes [1], the factors governing the distribution of cholesterol in membranes [2,3], as well as the existence of more than one pool of cholesterol in cells [4,5]. Moreover, almost nothing is known about the origin of the large distribution differences between cell membranes [6].

In order to investigate the formation of complexes between cholesterol and lipids or proteins, or the mechanism of its exchange between cell membranes, many analogues of cholesterol have been synthesized, including radiolabeled, fluorescent [7,8], ^{13}C spin labeled [9] and paramagnetic [10–12] probes. The paramagnetic analogues of cholesterol are particularly interesting since the ESR time scale (between 10^{-9} and 10^{-3} s) is convenient for determining when a small molecule forms complexes with larger systems. However, as in every probing method, it is important to known whether the labeling prevents

Abbreviations: TLC, thin-layer chromatography; DMPC, dimyristoylphosphatidylcholine; MLV, multilamellar vesicle; SUV, small unilamellar vesicle; CNO, 25-doxyl cholesterol; ESR, electron spin resonance; Tri-Sil TBT, a powerful silylating mixture composed of *N*-trimethylsilylimidazole/*N*,*O*-bis(trimethylsilyl)acetamide/trimethylchlorosilane.

Correspondence: A. Bienvenue, Laboratoire de Biologie Physico-chimique (UA 530 CNRS), USTL, F-34060 Montpellier cedex, France.

the analogue from correctly mimicking the behaviour of genuine cholesterol. Many paramagnetic components used until now have been inadequate in this respect since cholesterol loses some very important parts of its structure (hydrophobic tail, 3-hydroxyl group or 5-6 double bond) which often condition its reactivity. Recently, a paramagnetic analogue of cholesterol was synthesized by Keana et al. [12] by adding the nitroxide-containing ring after the D ring, without significantly disturbing the molecular properties of cholesterol.

In this paper, we describe the synthesis of a new paramagnetic analogue of cholesterol with nitroxide at the end of the tail (see formula B below).

We verified that the analogue possesses the same properties as genuine cholesterol in three respects: (i) its physical orientation in membrane as seen by ESR spectroscopy; (ii) its effect on the transition temperature of dimyristoylphosphatidylcholine (DMPC) as measured by ESR and Raman spectroscopy; (iii) its effect on the permeability properties of phospholipid membrane containing polyene antibiotics such as amphotericin B and filipin, as seen by fluorescence spectroscopy. In another paper (Lange, R, Maurin, L., Larroque, C. and Bienvenue, A., submitted to J. Biol. Chem.), we describe the evidence that this paramagnetic cholesterol is a good probe of cholesterol–cytochrome *P*-450 $_{scc}$ (side chain cleavage) interactions.

An ESR study of molecular interactions between this new compound and some polyene antibiotics is in preparation.

Materials and Methods

Chemicals. Egg phosphatidylcholine (type III E), DMPC (98%), amphotericin B, filipin and ergosterol were purchased from Sigma. Cholesterol was generously donated by Laboratory l'Oreal; 27-nor-5-cholestene-3β-ol-25-one was obtained from Steraloids Inc; 2-amino-2-methyl-1-propanol (99%), *m*-chloroperbenzoic acid, TLC plates (KieselGel 60/KieselGur F254), and calcein were from Merck.

Miscellaneous. Measurements were done on a NMR Brucker WR 300 S/Y apparatus, on a Jeol JMS-DX 300 mass spectrometer and on a Perkin-Elmer 457 infrared spectrometer.

Raman spectroscopy experiments. Raman spectra were displayed on a OMAR 89 apparatus from Dilor-France interfaced with an Apple IIe microcomputer. The sample (about 50 mg/ml lipid in water, in the form of MLV) was irradiated by an Ar^+ Spectra-Physics, model 2020-03 laser (500 mW at 514.5 nm). The spectrum, centered on 2900 cm^{-1} was obtained by retrospectroscopy on sedimented vesicles in 50 μl cuvettes thermostated ($\pm 0.2°$ C) in a home-made device. After base-line correction, the amplitude ratios of the characteristic lines were computed.

ESR spectroscopy experiments. Oriented samples were obtained essentially as described by Oehlschlager et al. [13], by a very slow drying of a water suspension of sonicated SUV on quartz plates. Nonoriented spectra were obtained in flat quartz cells with a thermoregulated device ($\pm 1°$ C). The ESR spectrometer was a Brucker ER 200D apparatus, interfaced with an Apple II^+ microcomputer.

Permeability studies. Liposome SUV suspensions were prepared by dissolving known amounts of phospholipids and sterol in chloroform. After removal of the solvent, these lipids were suspended in 300 μl, 10 mM Tris buffer (pH 7.4) (150 mM NaCl, 100 mM calcein), with a Vortex mixer and sonicated for 15 min at 4° C, or 20 min at 37° C if cholesterol was present with a Branson B-30 sonifier. After sonication, external calcein was eliminated by gel filtration (ACA 202 column, 1.2×10 cm). The total concentration of phospholipids in the new suspension was determined by total phosphate titration and sterol concentration by gas chromatography on a Girdel 300 apparatus, after derivation with Tri-Sil®/TBT (Pierce).

Fluorescence experiments. Calcein fluorescence was measured (490 nm excitation, 520 nm emission) with a Jobin Yvon JY3 apparatus as follows: 15 μl of vesicle suspension (75 nmol of phospholipids) were diluted with 1.5 ml of Tris buffer; the desired amount of amphotericin B or filipin was added from a freshly made solution 2 mg antibiotic/ml dimethyl formamide (DMF). For measurements with amphotericin B, 40 nmol of cobalt chloride solution were added. All experi-

ments were carried out at room temperature.

Synthesis. 27-Nor-25-doxyl-3-β-ol-5-cholestene (hereafter called CNO) was performed from 27-nor-5-cholestene-3β-ol-25-one essentially as described by Keana et al. [14]. The first step was the condensation of the 25-keto derivative with 2-amino-2-methyl-1-propanol to give an unstable oxazolidine 25-ring (A). A was then oxidized very gently with *m*-chloroperbenzoic acid in chloroform at 0 °C. The reaction was stopped by pouring into an aqueous hydrogen carbonate solution, when the oxazolidine derivative had disappeared, as checked by TLC (chloroform/ethyl acetate (84 : 16, v/v) as an eluant). A small amount (less than 20%) of another compound (presumably the 5,6-epoxide derivative) appeared in this procedure.

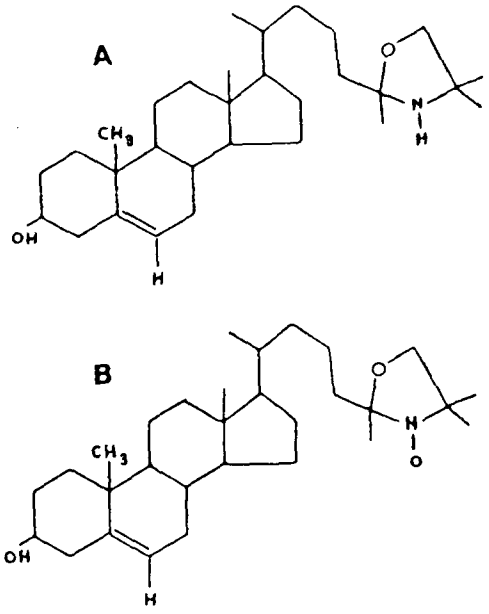

The CNO compound B was finally purified by HPLC (inverted phase C_{18} column on a Waters apparatus) by elution with an acetonitrile/water (86 : 14, v/v) mixture. The CNO chemical structure was assessed by spectroscopic methods. Infrared spectroscopy gave: NO (1365 and 1380 cm^{-1}) and OH (broad band around 3400 cm^{-1}). ^{1}H-NMR spectroscopy showed easily identifiable peaks among others shifted by paramagnetic effect provoked by the nitroxide radical : 19, CH_3 1.04 ppm; 21, CH_3 1.6 ppm; 6 H 5.35 ppm with the expected 1/3 ratio of H signal to the CH_3 signal. Mass spectroscopy showed a molecular peak at $m/z = 472$ and two other main peaks corresponding to the doxyl ring cleavage producing the 25-oxo derivative ($m/z = 386$), and to the side chain cleavage and loss of H_2O ($m/z = 255$).

Results

Orientation of CNO in model membrane

Three experiments were undertaken to show that cholesterol was perpendicular to membrane plane. Fig. 1 shows the ESR spectra of CNO included in oriented multilayers of phosphatidylcholine. The difference between the two spectra can be characterized by three parameters ($T'_{\parallel} = 18.1$ G; $T'_{\perp} = 12.4$ G, $\Delta H' = 2.5$ G), where T' and $\Delta H'$ represent the effective hyperfine parameters (symbols $\parallel$ and $\perp$ refer to the direction of the nitroxide π^* orbital with respect to the main magnetic field). These three values are related to the residual distribution anisotropy of the probe in the membrane [15], due to the fast movement of the hydrophobic tail of CNO. As expected, the two T' values were not very different, and the CNO order parameter [16] was almost the same ($S = 0.22$) as what was observed in the same membrane with a fatty acid probe spin labelled near the ω end of the tail ($S = 0.25$, not shown). From these values, a theoretical non-oriented spectrum could be computed [17]. Fig. 1 shows that experimental and calculated spectra are in very good agreement.

Another way to prove that CNO is oriented so that the doxyl ring is completely buried in the bilayer center, is to check the accessibility of the free radical by water soluble molecules. It is well known that ascorbate ions do not penetrate the membrane below 4 °C [18]. At this temperature, the amplitude of the ESR signal of diluted CNO (CNO/egg phosphatidylcholine, molar ratio 1 : 200) in sonicated vesicles was not reduced by 10 mM ascorbate for 1 h (not shown). Indeed, the same result was obtained at 37 °C.

CNO effect on phospholipid phase transition

Perhaps the most documented effect of cholesterol on membrane is the stabilization of its fluidity (for a review, see Refs. 6,20). By different spectroscopic and calorimetric techniques, the

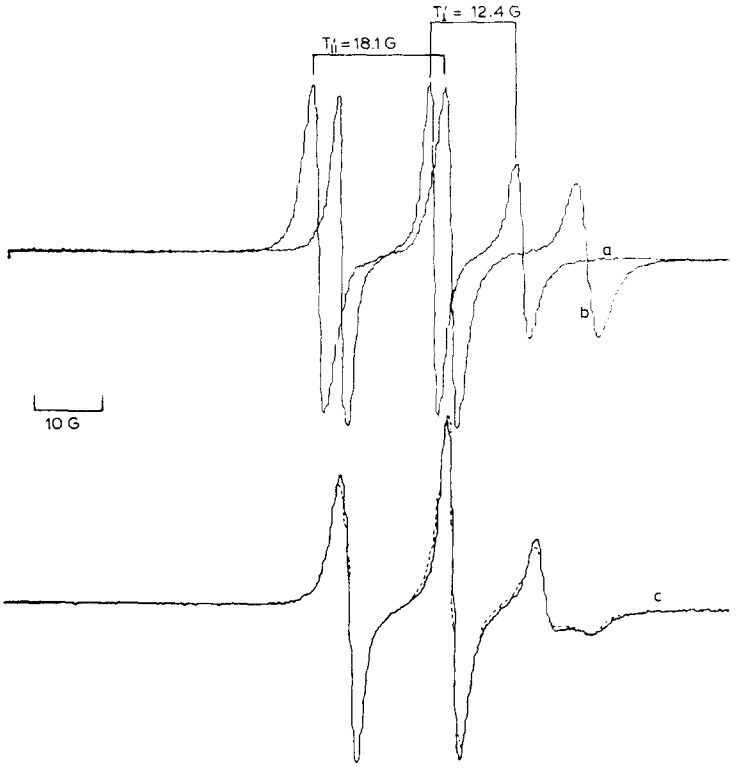

Fig. 1. ESR spectra of oriented egg phosphatidylcholine multilayers containing CNO at the 1:2500 molar ratio, with magnetic field perpendicular (a) or parallel (b) to the supporting plate. Spectrum (c) corresponded to non-oriented sample: (———) experimental; (— — —) calculated with the $T'_{\perp}$ and $T'_{\parallel}$, and $\Delta H'$ reported in the text, with the following widths for the low (1), middle (0) and high (−1) field peaks, in Gauss: $LW_{\perp}(1) = 1.4$; $LW_{\perp}(0) = 1.3$; $LW_{\perp}(-1) = 2.0$; $LW_{\parallel}(1) = 1.9$; $LW_{\parallel}(0) = 1.8$; $LW_{\parallel}(-1) = 2.2$, according to the results of spectra (a) and (b).

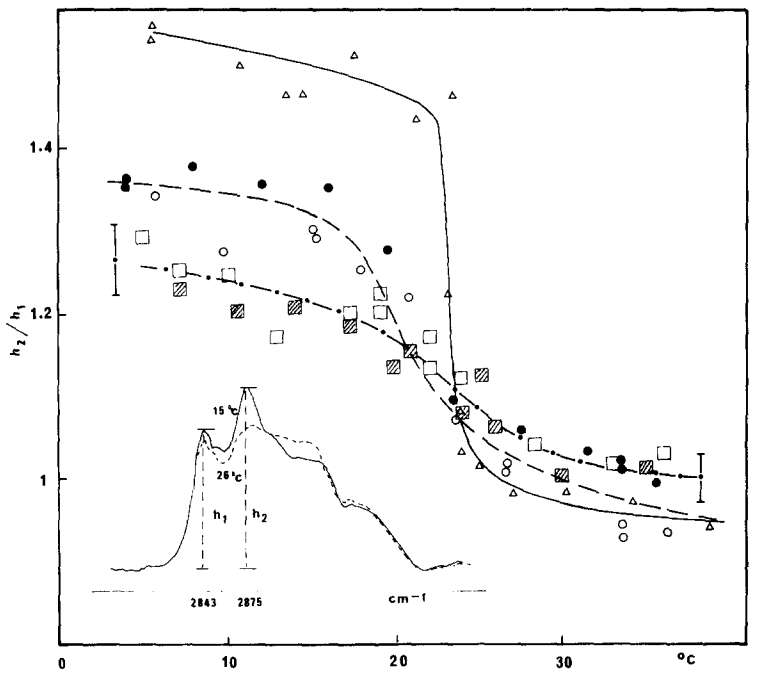

Fig. 2. Comparison of CNO and cholesterol effect on C–H stretching band intensity by Raman spectroscopy. Amplitude ratio (see inset for definition of h_1 and h_2) versus temperature for pure DMPC (△), CNO/DMPC (○), cholesterol/DMPC (●) 1:50 molar ratio and CNO/DMPC (□), cholesterol/DMPC (■), 1:5 molar ratio. Inset: experimental Raman spectra of pure DMPC MLVs, above (- - - - - -) or below (———) the transition temperature. Mean error bars are shown at extreme temperatures.

condensing and fluidizing effects of cholesterol have been clearly established in model systems and biological membranes. As a general rule, cholesterol provokes an increase in membrane fluidity below the transition temperature, but a decrease above. It was thus very important to check the effect of CNO on the phase transition of the phospholipid bilayer. We chose to do this by observing the ratio of two C-H stretching Raman band intensities (at 2843 and 2875 cm^{-1}) since it has been shown that this ratio clearly depends on the physical state of the hydrophobic fatty acid tail in membranes [20]. As shown in the inset in Fig. 2, the ratio of the band heights h_1 and h_2 from pure DMPC MLV was higher above the transition temperature (23°C) than below. The complete variation of this ratio is displayed in Fig. 2 as a function of temperature, with MLV containing either pure DMPC, or cholesterol/DMPC or CNO/DMPC in molar ratio of 1:50 or 1:5, respectively. In the limit of our experimental error variation, the temperature dependance of the h_2/h_1 ratio is identical whether DMPC is supplemented with CNO or with cholesterol. This suggests a very similar CNO and cholesterol effect on lipid phase transition.

In another approach, the ESR spectra of CNO in DMPC MLV (Fig. 3, inset) showed that the signal amplitude was clearly lowered by decreasing the temperature below the transition temperature. The H_1 amplitude can be used to characterize the effects (Fig. 3), H_1 varied identically with CNO/DMPC ratios of 1:2500 and 1:50. With a ratio CNO/DMPC of 1:5, broadened spectra were obtained and H_1 measurements are not comparable (not shown).

From the Raman and ESR studies, we can conclude that CNO acta on the phospholipid phase state like cholesterol itself.

Membrane permeability enhancement by CNO interaction with polyene antibiotics

One of the most studied molecular interactions of cholesterol is that occurring with polyene antibiotics (for a review, see Ref. 21). The main effect of this interaction on membrane is an increasing permeability for different kinds of molecules. This point is discussed more completely in the compa-

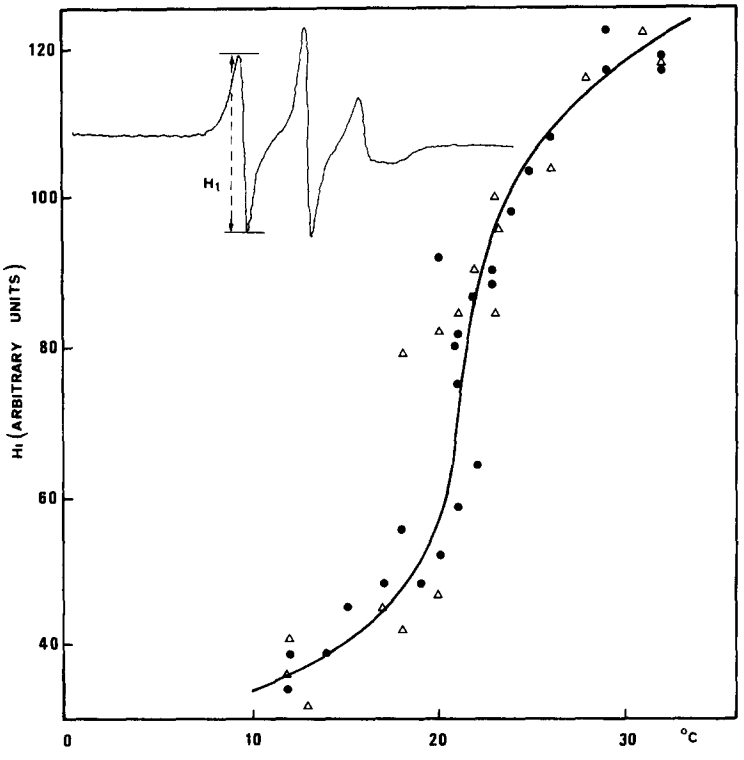

Fig. 3. Detection of DMPC phase transition by ESR spectroscopy of CNO, above or below the transition temperature. Variation in amplitude H_1 (see inset for definition of H_1) versus temperature, for CNO/DMPC molar ratios of 1:2500 (△), 1:50 (●). Inset: experimental spectra of CNO in DMPC vesicles.

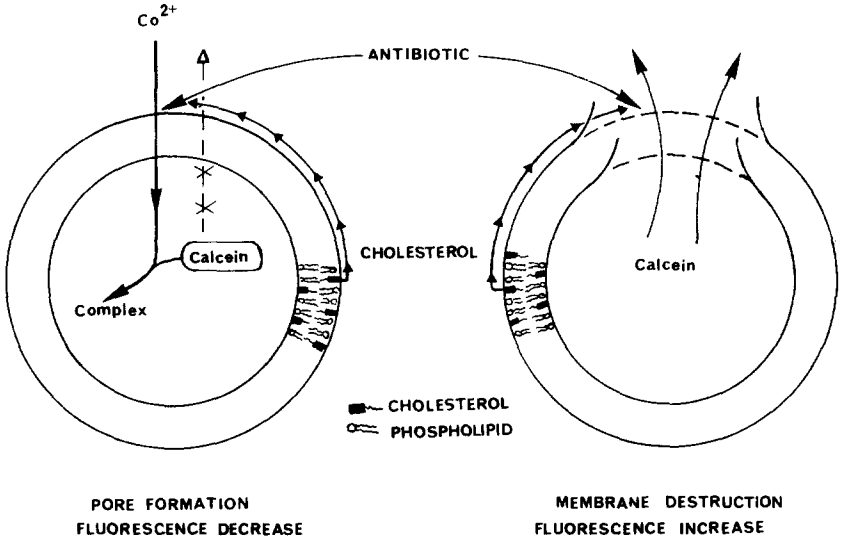

Scheme I.

nion paper. As a rule, however, permeability is relatively specific for small molecules or ions with the cholesterol–amphotericin B interaction while cholesterol-containing membranes tend to disrupt when filipin is added. In the present paper, we describe a new method, based on fluorescence measurements, to prove that CNO and cholesterol interact similarly with these antibiotics, at least with respect to permeability. This method is based on two different properties: (i) the well-known self-quenching effect of high concentrations of calcein and (ii) the cobalt quenching of calcein fluorescence, which is easily measurable because of the very high affinity of these two particles. The principle of the method is described in Scheme I.

A high concentration of calcein is enclosed in cholesterol- or CNO-containing SUV, thus giving a relatively low fluorescence yield. With the addition of an antibiotic, permeability increases. If calcein cannot cross the membrane, while cobalt can (for example because of pore selectivity), an addition of cobalt outside the vesicle must produce a decrease in fluorescence intensity as soon as cobalt enters the vesicles. On the other hand, if calcein is able to cross into the outside medium and become diluted, a large increase in fluorescence follows the addition of antibiotic, when no cobalt is added.

As seen in Fig. 4A, the addition of amphotericin B to calcein-containing vesicles did not modify the fluorescence of the sample, showing that calcein did not leak into the external medium. By contrast, after the addition of cobalt, a fast fluorescence quenching occured until the fluorescence reached a plateau. This means that cobalt entered the vesicles, presumably because it is smaller than calcein. The position of this plateau depended in a saturable manner on the amount of amphotericin B added. The plateau reached at very high amphotericin B concentrations was near the fluorescence level obtained after the addition of Triton X-100, which completely dissociated the liposomes. There was a cobalt-provoked fluorescence decrease even in the absence of amphotericin B, obviously because part of the observed fluorescence came from a small amount of nonenclosed calcein. The same kind of experiments were reproduced with different sterol/phospholipid ratios and with different kinds of sterols, namely cholesterol, CNO, and ergosterol. The plateau position, relative to the maximum observable effect (see Fig. 4A for a definition of the parameters ΔF and ΔF_{max}), is plotted in Fig. 4B versus the amphotericin B/sterol molar ratio. The curves were hyperbolic in shape. On the other hand, the saturation effect was reached with a lower

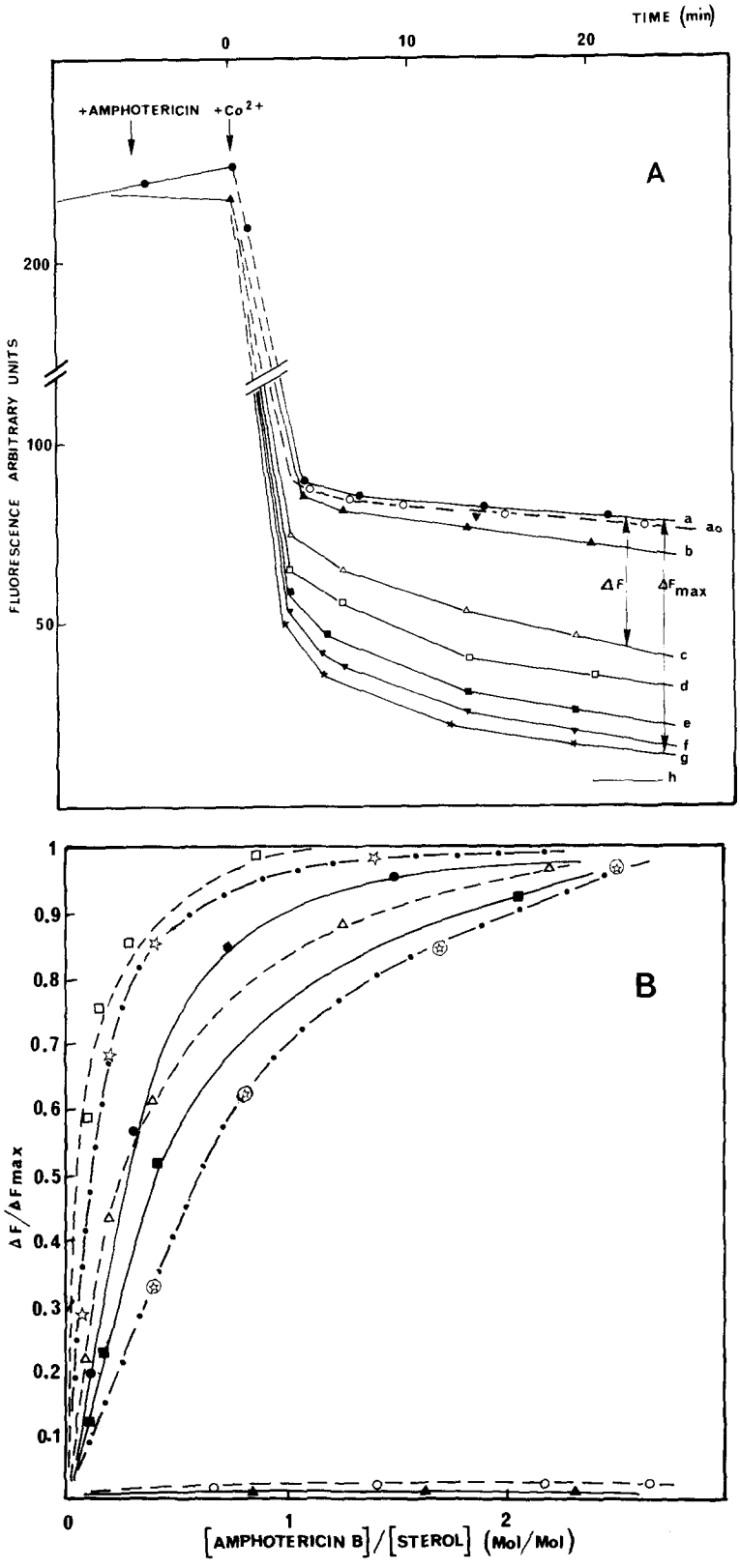

Fig. 4. Fluorescence study of amphotericin B induced enhancement of membrane permeability. (A) Fluorescence intensity of entrapped calcein (100 mM internal concentration) in cholesterol/egg phosphatidylcholine (1 : 4 molar ratio) vesicles (55 μM in phospholipid) after addition of amphotericin B, then 5 min later of cobalt ion (30 μM final). The added amphotericin B was at the following final concentration (μM): (a) 0; (b) 1; (c) 5; (d) 10; (e) 15; (f) 20; (g) 30. a_0 is control without cholesterol in vesicles treated or not by amphotericin B. The last position (h) was obtained after addition of Triton X-100 (0.01% final concentration). (B): Effect versus amphotericin B/sterol molar ratio plot. ΔF and ΔF_{max} were defined in part A. The sterol concentrations were CNO: (□) 12 μM; (△) 6 μM; (○) 2 μM; cholesterol: (●) 10 μM; (■) 3 μM; (▲) 1 μM; ergosterol: (☆) 13 μM; ((☆)) 0.6 μM.

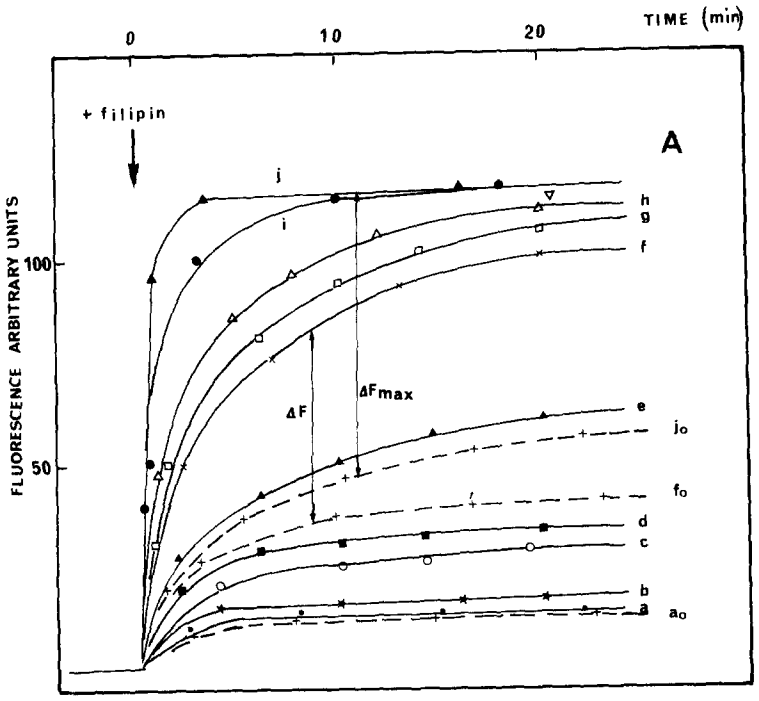

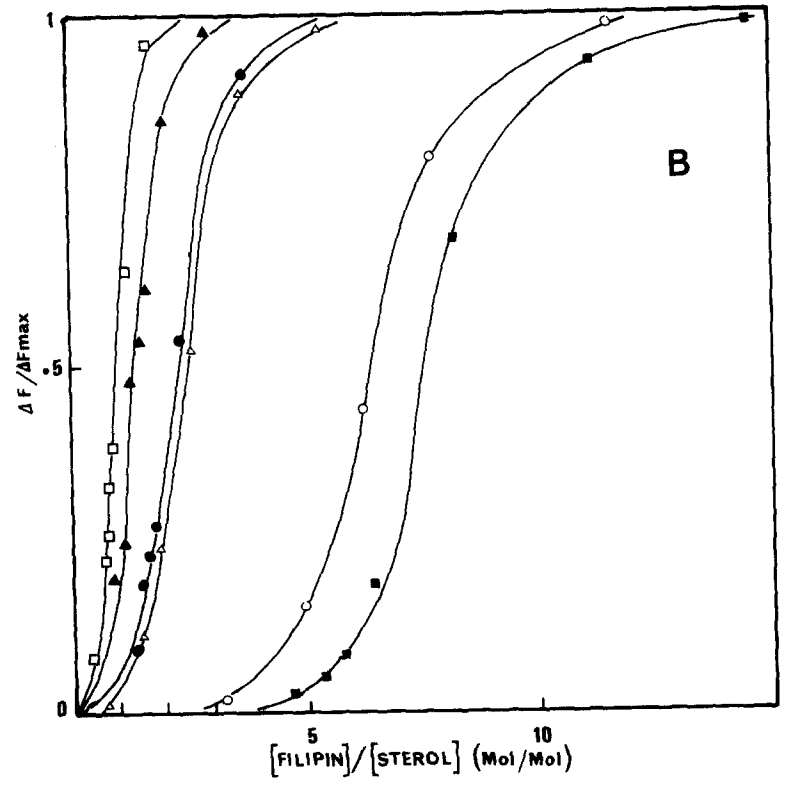

Fig. 5. Fluorescence study of filipin induced enhancement in membrane leakage. (A) Fluorescence intensity of calcein (100 mM) initially entrapped in cholesterol/egg phosphatidylcholine (1 : 4 molar ratio) vesicles (55 μM in phospholipid) in solid lines or vesicles without cholesterol in dashed lines (and index o), after addition at time zero of filipin at final concentrations (in μM): (a) 0; (b) 4; (c) 5; (d) 6.6; (e) 8; (f) 9; (g) 10; (h) 11; (i) 14 and 20; (j) 0 but 0.01% Triton-X-100. (a_0) 0; (f_0) 9; (j_0) 20. (B) Effect versus filipin/sterol molar ratio plot. ΔF and ΔF_{max} were defined in part A. The sterol were CNO: (□) 12 μM; (△) 6 μM; (○) 2 μM; cholesterol: (▲) 7 μM; (●) 6 μM; (■) 1.7 μM.

amphotericin B/sterol ratio when the sterol/phospholipid ratio was higher, quite independent of the chemical structure of the sterol.

The results were quite different when filipin was added to calcein-containing vesicles. Filipin in fact provoked a fast and large fluorescence increase, corresponding to a leakage of calcein, either through the membrane or by disruption (Fig. 5A). Here again, a plateau was reached in 10–20 minutes, its position depending on the added filipin concentration. Moreover, a very high concentrations of filipin gave the same fluorescence enhancement as Triton X-100, which completely disrupted the vesicles. In Fig. 5B, the plateau position ΔF, relative to the maximum observable effect ΔF_{max} is plotted versus the filipin/sterol molar ratio. The curves seem much more cooperative in this case than with amphotericin B (Fig. 4B), showing a threshold concentration of filipin which decreases as the sterol/phospholipid molar ratio increases in the vesicle membrane.

Discussion

This work provides good evidence that CNO can be used to report the physical behavior and molecular associations of cholesterol, at least in three respects. The first is related to the molecular distribution in the phospholipid bilayer. ESR spectra of CNO in oriented multilayers (Fig. 1) as well as the nonreactivity of the nitroxide moiety with a water soluble reactant such as ascorbate, indicate that CNO is arranged in the membrane, perpendicular to its mean plane, with the hydroxyl group near the aqueous phase, exactly like cholesterol itself, as observed by many differents physical methods (for a review, see Ref. 6). The order parameter computed from ESR spectroscopy at C-25 (0.22) is different from the one ($S = 0.66$) computed at C-24 by Dufourc et al. [22] from H^2-NMR experiments. Besides the fact that the two values are not related to the same carbon atom, the difference could be due to one or all of the following three effects: (i) the known effect of a doxyl ring on order parameter [23]; (ii) a relative large (20–40°) angle between the orbital axis and the axis of segmental motion [24]; (iii) an 'immobilizing' effect on the hydrophobic tail when a large cholesterol concentration is used for NMR experiments.

The second is related to the organizing effect of cholesterol on fatty acid chains in phospholipid membranes. It must be emphasized that this point was checked by method other than ESR, namely Raman spectroscopy, to ensure that the observation of the probe properties did not influence the measurement itself. As shown in Fig. 2, the CNO and cholesterol effects on DMPC phase transition are nearly identical, as far as the *trans/gauche* conformational ratio is concerned [19]. This point was confirmed by the ESR spectra (Fig. 3). The expected effect of a temperature decrease on reducing the movement of the probe, was a decrease in the overall spectrum, which was exactly the same for CNO/phospholipid ratios of 1:2500 and 1:50.

The third point studied here concerns the evidence that CNO can mimic correctly cholesterol in its interactions with polyene antibiotics. The leakage of small ions (cobalt) or of a larger molecule (calcein) was used to determine whether CNO interacts with these antibiotics. As expected, the two antibiotics did not have the same effect.

Amphotericin B is known to increase the permeability of the membrane quite specifically for small molecules or ions [25,26]. For example, it is well known [26,27] that H^+ and K^+ can cross amphotericin-B-treated membranes, like cobalt, as shown in Fig. 4A. By contrast, slightly larger molecules like glucose (and calcein, as shown in Fig. 4A) cannot cross these membranes. With filipin, our results reported in Fig. 5A are in agreement with a complete disruption of the membrane by interaction between sterols and the antibiotic. The other difference between the two antibiotics consists on the shape of the dose effect curve. With amphotericin B, a simple equilibrium constant could be used to characterize the interaction with sterol. However, we did not attempt a more precise interpretation of these results because it has been shown by Bolard et al. [28] that the actual concentration of amphotericin B in membrane is very difficult to determine, since it also exists in many other states, such as pure amphotericin B or phospholipid-mixed micelles, and aqueous sterol-amphotericin B complexes. With filipin, the dose-effect curves are much more cooperative (Fig. 5B) probably because an association between several components is needed to

cause the leakage of calcein into the external medium, presumably by disruption of the membrane [29]. When the sterol concentration was high in membrane, the threshold filipin/sterol molar ratio was around 1, but it increased considerably when the sterol was less abundant. Larger amounts of either antibiotic were needed to provoke a given effect when the sterol/phospholipid molar ratio was lower, as expected by the mass action law. Amphotericin, however, needed much more sterol in membranes than filipin to provoke a measurable effect (Figs. 4B, 5B). Furthermore, with the two antibiotics, the antibiotic/sterol ratio resulting in a leakage is almost the same, with CNO and with cholesterol (Figs. 4B, 5B). As already observed the interaction between amphotericin B and ergosterol is greater than with cholesterol and, as we saw, with CNO.

To summarize, CNO can quite precisely mimic genuine cholesterol in three of its molecular effects in membrane. As mentioned above, CNO is also a good indicator of the interactions of cholesterol with cytochrome $P\text{-}450_{scc}$, an enzyme from adrenal cortex mitochondria [4]. Thus, this paramagnetic compound can be used to study many molecular properties of cholesterol by ESR spectroscopy (such as lateral and transverse diffusion rates in membrane, exchange between membranes either in one cell type or between two different ones, etc.), with the assurance that the results obtained with this probe can reasonably be transferred to cholesterol itself.

Acknowledgements

The authors thank Miss M. Fize for editorial assistance; Dr. P. Bette-Bobillo and Dr. R. Lange for critically reading the manuscript; Mr. J. Goodfellow for english translation assistance.

References

1 Quin, P.J. (1981) Prog. Biophys. Mol. Biol. 38, 1
2 Van Dijk, P.W.M., De Kruijff, B., Van Deenen, L.L.M., De Gier, J. and Demel, R.A. (1976) Biochim. Biophys. Acta 455, 576–587
3 Blume, A. (1980) Biochem. 19, 4908–4913
4 Lange, Y., Cutler, H.B. and Steck, T.L. (1980) J. Biol. Chem. 255, 9331–9336
5 Bloj, B. and Zilversmit, D.B. (1982) J. Biol. Chem. 257, 7608–7614
6 Yeagle, P.L. (1985) Biochim. Biophys. Acta 822, 267–287
7 Anderson, R.G.W., Goldstein, J.L. and Brown, M.S. (1980) J. Receptor Res. 1, 17
8 Derzko, Z. and Jacobson, K. (1980) Biochemistry 19, 6050
9 Yeagle, P.L. (1981) Biochim. Biophys. Acta 640, 263–273
10 Seigneuret, M., Favre, E., Morrot, G. and Devaux, P.F. (1985) Biochim. Biophys. Acta 813, 174–182
11 Aracava, Y., Smith, I.C.P. and Shreier, S. (1981) Biochemistry 20, 5702–5707
12 Keana, J.F., Tamura, T., McMillen, D.A. and Jost, P.C. (1981) J. Am. Chem. Soc. 103, 4904–4912
13 Oehlschlager, A.C. and Laks, P. (1980) Can. J. Biochem. 58, 978–985
14 Keana, J.F., Keana, S.B. and Beethmam, D. (1967) J. Am. Chem. Soc. 89, 3055–3056
15 McConnell, H.M. and McFarland, B.G. (1972) Ann. N.Y. Acad. Sci. 195, 207–217
16 McConnell, H.M. (1976) in Spin Labeling, Theory and Applications (Berliner, L., ed.), pp. 525–560, Academic Press, New York
17 Davoust, J. and Devaux, P.F. (1982) J. Magn. Reson., 48, 475–494
18 Kornberg, R.D. and McConnell, H.M. (1971) Biochemistry 10, 1111–1120
19 Anthony, T.Tu. (1982) Raman Spectroscopy in Biology, Wiley-Interscience Publication, pp. 187–233
20 Wallach, D.F.H., Verma, S.P. and Fookson, J. (1979) Biochim. Biophys. Acta 559, 153–208
21 Demel, R.A., Crombag, F.J.L., Van Deenen, L.L.M. and Kinsky, S.C. (1968) Biochim. Biophys. Acta 150, 1–14
22 Dufourc, E.J., Parish, E.J., Chitakorn, S. and Smith, I.C.P. (1984) Biochemistry 23, 6062–6071
23 Seelig, J. and Niederberger, W. (1974) Biochemistry 13, 1585–1588;
24 Seelig, J. (1976) in Spin Labeling, Theory and Applications (Berliner, L., ed.), pp. 373–409, Academic Press, New York
25 Vertu-Croquin, A., Bolard, J., Chabert, M. and Gary-Bobo, C.M. (1983) Biochemistry 22, 2939–2944
26 De Kruijff, B., Gerritsen, W.J., Oerlemans, A., Van Dijck, P.W.M., Demel, R.A. and Van Deenen, L.L.M. (1974) Biochim. Biophys. Acta 339, 44–56
27 De Kruijff, B., Gerritsen, W.J., Oerlemans, A., Demel, R.A. and Van Deenen, L.L.M. (1974) Biochim. Biophys. Acta 339, 30–43
28 Bolard, J., Seigneret, M. and Boudet, G. (1980) Biochim. Biophys. Acta 599, 280–293
29 Van Zutphen, H., Demel, R.A., Norman, A.W. and Van Deenen, L.L.M. (1971) Biochim. Biophys. Acta 241, 310–330